

MULTIBODY COMPUTATIONAL BIOMECHANICAL MODEL OF THE UPPER BODY

Sarah R. Sullivan

Rutgers, The State University of New Jersey
Biomedical Engineering
617 Bowser Road
Piscataway, New Jersey, 08854
USA
(732)-445-3155
sarsulli@eden.rutgers.edu

Noshir A. Langrana

Rutgers, The State University of New Jersey
Biomedical Engineering/
Mechanical and Aerospace
Engineering
98 Brett Road
Piscataway, New Jersey, 08854
USA
(732)-445-3618
langrana@rutgers.edu

Sue Ann Sisto

Human Performance and
Movement Analysis Laboratory
Kessler Medical Rehabilitation and
Research Education Corporation
1199 Pleasant Valley Way
West Orange, New Jersey
07052 USA
(973)-243-6888
ssisto@kmrrec.org

ABSTRACT

In the United States alone, more than 10,000 spinal cord injuries (SCI) are reported each year. This population depends upon their upper limbs to provide a means of locomotion during completion of their activities of daily living. As a result of greater than normal usage of the upper limbs, proper propulsion mechanics are paramount in preventing injuries. Upper limb pain and pathology is common among manual wheelchair users due to the requirements placed on the arms for wheelchair locomotion. During the wheelchair rehabilitation process following an SCI, an individual is prescribed a wheelchair (WC). The use of a *patient-specific* computational biomechanical model of WC propulsion may help guide rehabilitation that may improve clinical instruction and patient performance. The overall goal of this study is to develop and refine a computational model that may aide in minimizing shoulder pathology.

KEYWORDS

Biomechanics, computational modeling, shoulder, kinematics, kinetics, inverse dynamics, optimization.

INTRODUCTION

Researchers have studied the biomechanical factors involved during standard WC propulsion [1-3]. It has long been thought that prolonged WC use and transfers cause the high frequency of upper limb cumulative trauma and strain injuries in individuals with an SCI [4]. Such trauma, like

glenohumeral joint impingement, has been quantified using radiographic data from both cadaveric and healthy volunteers [5-7]. Cross-sectional studies have reported the prevalence of shoulder pain in individuals with SCI to be between 42% and 73% [8, 9]. Such studies illustrate the importance of good muscular strength, muscular endurance, and proper biomechanics in maintaining the integrity of the musculoskeletal system of WC users as they perform activities of daily living.

To this point, very few shoulder models exist, and even less have the flexibility to be made patient-specific. The complexity of the shoulder coupled with its multiple degrees of freedom has historically presented modeling problems.

OBJECTIVES

The major effort is to build a computational model of wheelchair propulsion biomechanics to predict optimal forces, muscle activity, and seat position. The overall goal of this study is to develop and refine a computational model to minimize shoulder pathology; the use of a computational biomechanical model of WC propulsion may help guide rehabilitation that may improve clinical instruction and patient performance.

MODEL

The current model includes the upper body with all surrounding muscle groups. Using the gait analysis data that we

have from each individual, including the subject's kinetic data from force-sensing push-rims, kinematics, and patient-specific anthropometrics, the muscle forces and joint reaction forces around all joints necessary to achieve the defined movement are computed through inverse dynamics analysis.

A patient-specific computational biomechanical model of the shoulder is constructed using the commercially available software developed by AnyBody Technology [10], Figure 1. This software allows the complete creation of a biomechanical model, including the model's interaction with the surrounding environment, in this case the wheelchair. The body part of the model consists of the upper body bone-tendon-muscle unit. The entire skeleton of the upper body has been included from the pelvis up. This includes, but is not limited to, the scapula, clavicle, sternum, humerus, radius, and ulna. To minimize computational stress, both legs have been excluded from the model as we feel their contribution to be negligible for what we are looking for. Future studies may include them for more complete results.

All corresponding musculature for the upper body is included as well, with particular focus on the following 15 muscles surrounding the shoulder: pectoralis (major and minor), deltoids, biceps brachii, triceps brachii, trapezius, latissimus dorsi, coracobrachialis, infraspinatus, levator scapulae, rhomboideus, serratus anterior, subscapularis, supraspinatus, teres major, and teres minor.

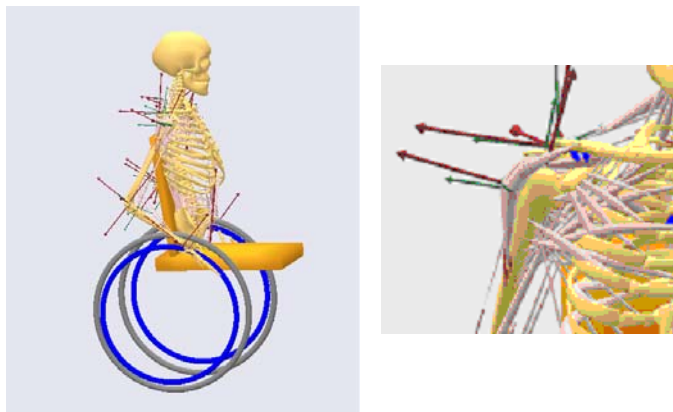


Figure 1: Current biomechanical computational model (left), with a zoomed-in view of the right shoulder (right).

The segment axes within the model correspond to the International Society of Biomechanics (ISB) standards [11]. In this system, positive-X is forward and horizontal (in the direction of wheelchair movement), positive-Y is up and vertical (the XY plane makes up the sagittal plane), and the positive-Z, according to the right-hand-rule, is to the right and horizontal, as shown in Figure 2.

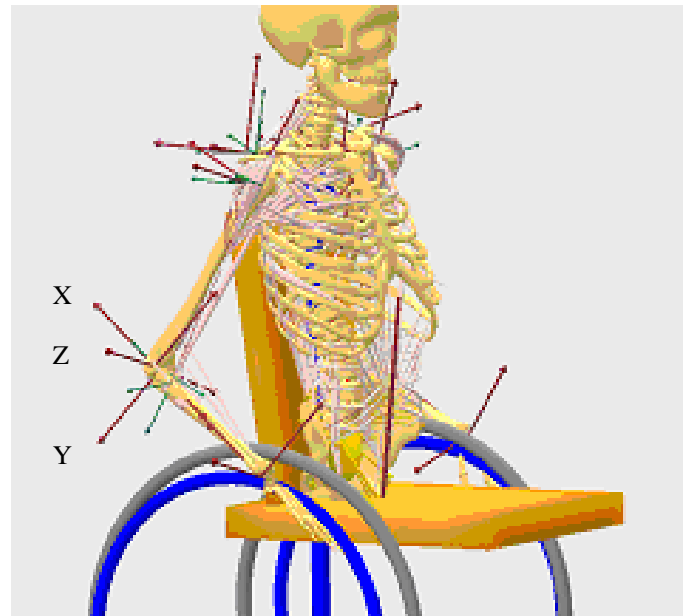


Figure 2: Joint axes labeled above in red. For ease in labeling, the labeled X- and Y- axes are actually negative.

Degrees of freedom of the system are set up as follows: for each defined segment in the model, there are a total of seven degrees of freedom, three displacement and four Euler parameters. The resulting seven equations for each segment are used to solve the rigid body dynamics problem. For the current set-up of a subject in their wheelchair, the degrees of freedom of the system are defined by:

- 3 degrees of freedom in each shoulder (6 total)
- 1 degree of freedom in each elbow (2 total)
- 2 degrees of freedom in each wrist (4 total)
- 1 degree of freedom in the wheelchair

With both hands on the wheelchair during the push phase of propulsion, the model is a closed kinematic chain. The degrees of freedom of the system are reduced, and kinematic indeterminacy is prevented. The range of motion is constrained by the defined kinematics movement, further reducing the degrees of freedom of the system, and the rigid body dynamics problem becomes unique.

MODEL FLEXIBILITY

The current model's segments follow rigid body dynamics concepts. All properties of the rigid-body bone geometries are controllable. The parameters in the current model are based on cadaver data, however the flexibility of the model allows for change of the current bone design. Simplistic anthropometric changes such as changing the length of the bone can be made, or the entire bone can be re-created for more patient-specificity.

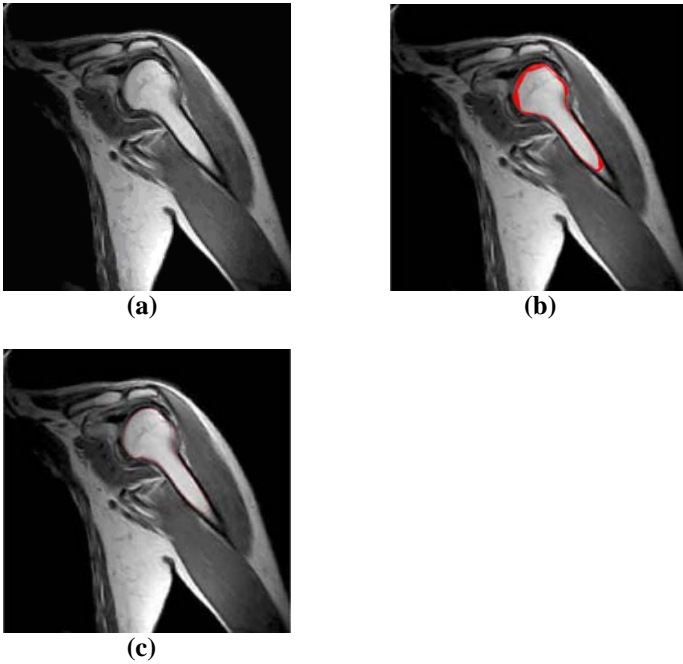


Figure 3: An example of a snake program being run. The overall goal of a snake program is edge detection between the bone and soft tissue. Far left: an original shoulder MRI. Center: the snake program in progress. Far right: the resulting outline of the humeral head. It can be seen that after 250 iterations, the snake program appears to have found an accurate representation of the boundary of the bone to aide in accurate geometrical calculations.

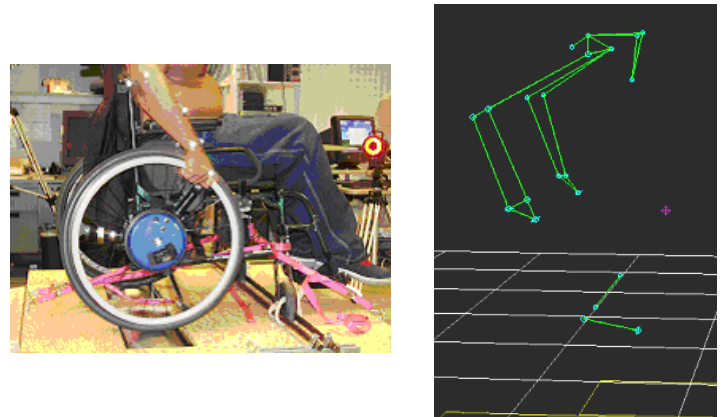
Patient MRI data can aide in the creation of further patient specificity within the model, Figure 3. The analysis of MRI data for exact patient bone geometries can be performed. By using an edge-detection snake program to segment patient MRI slices, a 3-D bone can be reconstructed in nearly any CAD program. The bone models are then exported in STL ASCII format and added to the AnyBody model. Patient-specific 3-D bone geometries of the entire upper body skeletal structure can be generated in this fashion.

Properties of muscle can be changed as well. Geometrical placement of muscle origin and insertion attachments can be changed to reflect a patient’s anatomy, data also found from MRI images. Muscle property data can be changed as well, such as the individual’s muscle physiological cross-sectional area (PCSA), isometric muscle force, nominal fiber length, and nominal pennation angle. The normalized maximum velocity of the muscle can also be changed, as well as the relative amount of “fast” fibers in the muscle. Tendons can also be accurately represented in the model, and the shape constant for the tendon, as well as the nominal tendon strain and tendon length can all be changed.

EXPERIMENTAL DATA

Figure 4 shows the set-up for kinematics and kinetic data collection. In an individual’s own wheelchair, with force-sensing push-rims swapped for their own, the subject’s back wheels are placed on rollers and the chair is fixed to the platform as shown below. Infrared cameras pick up the

kinematics data from the reflective markers (Figure 4) on the subject’s hand (1), wrist (2), elbow (2), and shoulder (1). While the cameras record the motion data (shown in Figure 5), the force-sensing push-rims collect the kinetic data.



Figures 4 (left) and 5 (right): Subject set-up for data collection (left). Corresponding regenerated stick figure kinematics of an individual pushing a wheelchair.

COMPUTATIONAL MODEL

Using kinetic data from force-sensing push-rims and anthropometrics data specific to each subject, joint reaction forces and moments are calculated up the arm by inverse dynamics. This data, coupled with the subject’s gait analysis kinematics data, can determine the muscle forces necessary to achieve the defined movement, assuming that muscles are recruited according to an optimality criterion.

The mathematical approach embedded within AnyBody Software assumes that minimizing maximal muscle activity is physiologically reasonable as it corresponds to a minimum fatigue criterion [12]. The problem of indeterminacy is achieved through an iterative solving technique, and a Numerical Recipes (NR) Simplex approach. At this point, the mathematical definition of the problem becomes [13]:

$$\text{Minimize } G(\mathbf{f}^{(M)}) \quad (1)$$

$$\text{Subject to } \mathbf{C}\mathbf{f} = \mathbf{d} \quad (2)$$

$$\frac{f_i(M)}{N_i} \leq \beta, i \in \{1, \dots, n(M)\} \quad (3)$$

$$f_i(M) \geq 0, i \in \{1, \dots, n(M)\} \quad (4)$$

Where G is the objective function of the recruitment strategy stated in terms of the muscle forces ($\mathbf{f}^{(M)}$) and minimized with respect to all unknown forces in the problem, $\mathbf{f} = [\mathbf{f}^{(M)T} \mathbf{f}^{(R)T}]^T$ ($\mathbf{f}^{(M)}$, and joint reactions, $\mathbf{f}^{(R)}$). Equation (2) is the dynamic equilibrium equation, which acts as a constraint in the optimization problem; \mathbf{C} is the coefficient-matrix for the unknown forces, and \mathbf{d} contains all known applied loads and inertia forces. The constraints (3) ensure that the only way to reduce the objective, β , is to simultaneously reduce all the relative muscle forces. The non-negativity constraints on the

muscle forces (4), state that muscles can only pull, not push [14].

The idea of optimization is based on the assumption that forces between different shoulder muscles are distributed consistently in similar tasks. AnyBody assumes that muscles are recruited according to an optimality criterion. This criterion distributes forces over redundant muscles to minimize the maximum muscle activation [15]. The optimality criterion defined within AnyBody is as follows:

$$G(\mathbf{f}^M) = \max \frac{(f_j)}{N_j} + \varepsilon_1 \sum \frac{(f_j)}{N_j} + \varepsilon_2 \sum \frac{(f_j)^2}{N_j}$$

The epsilon values, ε_1 and ε_2 , can be changed to meet different needs of the system. For example, by making ε_1 infinitely large, we can determine which muscles have the largest input into the system. Or by setting ε_1 and ε_2 to zero (neglecting fatigue), and solving the resulting objective function below, the optimization function solves for the maximum cooperation between muscles:

$$G(\mathbf{f}^M) = \max \frac{(f_j)}{N_j}$$

Adjustments of the epsilon values will be investigated in future studies, and the role that each muscle plays in the kinematically defined movement will be determined. Muscle recruitment patterns, as well as fatigue in an individual with a spinal cord injury (SCI), can be significantly different than that of their able-bodied counterparts, and significant analyses and situations will have to be considered in finding the optimal scenario for the most accurate patient-specific shoulder model.

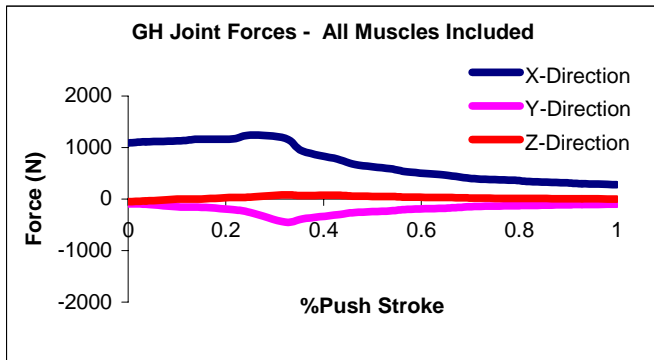


Figure 6: The shoulder joint forces for one complete push stroke when all corresponding muscles are included in the model (see model for specific muscles).

MODEL INPUT

A physiologically realistic and accurate model was created for a 50th percentile American male subject. The glenohumeral joint loads were computed for two wheelchair speeds of 0.9 m/s and 1.7 m/s (approximately 2 and 3.8 mph, respectively), and the torque applied to the wheels was 10 Nm. 0.9 m/s is considered to be a “leisurely” push speed, while 1.7 m/s is considered a more vigorous push. The entire push stroke in cycle is performed in 0.28 seconds at 0.9 m/s, and 0.15 seconds

at 1.7 m/s, to achieve 30° of wheel motion (hand-on at -15°, hand off a +15° from vertical). For comparison purposes between the two speed situations, the push stroke is normalized. Joint force changes were analyzed looking both at the differences in changing the speed of the push-stroke as well as under varying the muscle contributions of the upper body. In all cases, a feasible solution was achieved.

RESULTS

Muscle Dependence:

Previous studies have reported peak glenohumeral joint forces during the push phase to be between 800 and 1400 N, with quasistatic push phase forces being upwards of 2000 N [16-17]. The current model produced feasible results with calculated maximal glenohumeral joint reaction forces falling within this range. Figures 6 through 8 show joint reaction forces for one complete push-stroke. In all cases, the maximum joint reaction occurs in first 40% of the push stroke.

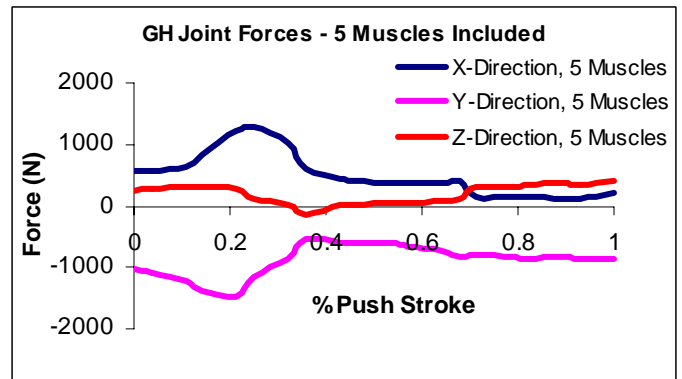


Figure 7: The shoulder joint forces for one complete push stroke when the pectorals, deltoids, biceps brachii, triceps brachii, and trapezius muscles are the only muscles included in the model.

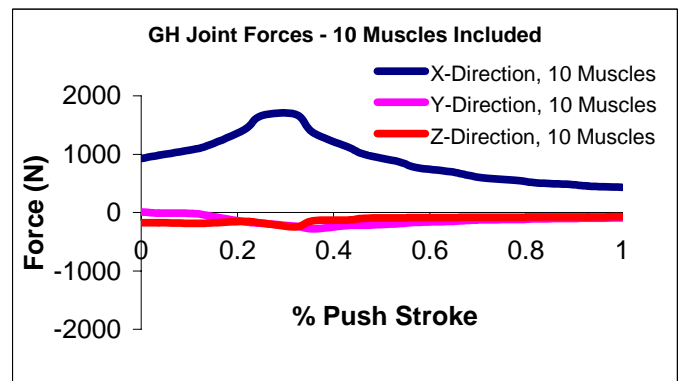


Figure 8: The shoulder joint forces for one complete push stroke when the latissimus dorsi, coracobrachialis, infraspinatus, levator scapula, rhomboideus, serratus anterior, subscapularis, supraspinatus, teres major, and teres minor muscles are the only muscles included in the model.

The joint forces are minimum, and the majority of the reaction appears to balance the external efforts in the direction of motion with all muscles contributing throughout the push (Figure 6), versus a push-stroke with only partial upper body muscle contribution (Figures 7 and 8). When the rotator cuff muscles are neglected in the model, the joint force in both the X- and Y-directions increase (Figure 7). This may imply that smaller muscle groups maintain stability in all three planes and provide a balanced joint reaction. When muscles with large, physiological cross-sectional areas are neglected (Figure 8), the maximal joint force in the X-direction again increases. A possible explanation may be that the smaller, rotator cuff muscles that surround the shoulder joint are compensating in the absence of the larger muscles, thus creating greater joint forces.

Velocity Dependence:

The peak joint force has been shown to increase by approximately by 7%, noticeably in both the X, and Z-directions, when the velocity of the push-stroke increases. All upper-body contributing muscles are included in the analysis. Figure 9, shown below, is the resulting graph after the velocity of the push-stroke has been increased from 0.9 m/s to 1.7 m/s, a more vigorous push.

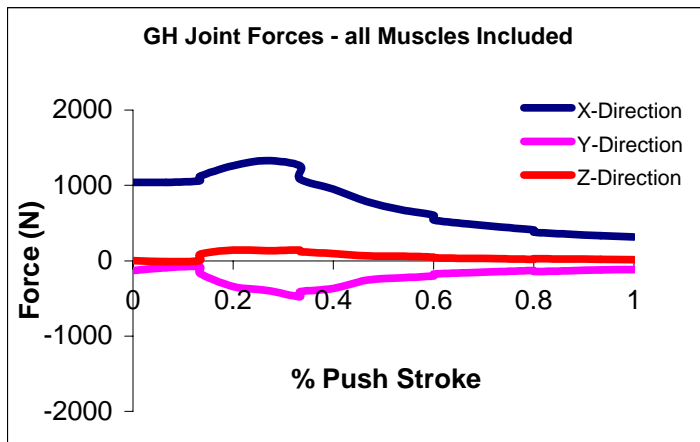


Figure 9: The shoulder joint forces for one complete push stroke when all muscles are included in the model, at an increased velocity of 1.7m/s.

DISCUSSION

Prolonged WC use and transfers have long been thought to cause the high frequency of upper limb cumulative trauma and strain injuries in SCI. Studies have also shown that push technique is an important factor in relation to shoulder injury, and illustrate the importance of good muscular strength, muscular endurance, and proper biomechanics in maintaining the integrity of the musculoskeletal system of WC users as they perform activities of daily living [1-9].

Model validation, an important part of data confirmation, can be achieved two different ways. First, because the model solves for muscle forces via an optimization technique previously discussed, EMG activity data collected

from the subject can be compared to the computed muscle activity in the model. While EMG data cannot quantitatively measure muscle force output, it can be used to validate the muscles involved in the movement, as well as the correlation between muscle firing patterns of the subject and model. Second, with correct muscle information, the model can further be validated using known wheel torque outputs. Wheel torque, coupled with the assumption that the muscle force output of the model is correct (from the initial validation), can be used as inputs into the model to calculate the kinetics required for the specified movements. The output kinetics can easily be validated with the data from the force sensing push-rims to assure further model accuracy.

Future work should focus on the model optimization, to potentially find an altered push-stroke that may in turn, minimize joint torque and potential shoulder injury. It may also be used to potentially overhaul current wheelchair design. An accurate model can be invaluable to both researchers and clinicians as together, achieving a better quality of life for those with a spinal cord injury is possible.

SUMMARY

Our current study has demonstrated the capability of a physiologically realistic multibody computational biomechanics model of the upper limb. Inverse dynamics computations are performed to estimate joint forces and muscle force contributions, under varying speed and muscle activity situations. In all circumstances, feasible solutions were obtained.

The accuracy of the model can be validated multiple ways through both EMG and torque data. To this point, very few shoulder models exist, and even less have the flexibility to be made patient-specific. The promise in this novel way of accurately modeling patient-specific biomechanics has boundless implications, including but not limited to the optimization of an individual's push-stroke for a better, pain-free, way of life.

ACKNOWLEDGMENTS

The first author was supported through funding from the National Science Foundation GK-12 Fellowship. This study was performed towards the partial fulfillment of the requirements for the degree of Doctor of Philosophy at Rutgers, The State University of New Jersey, for the first author. We would like to gratefully acknowledge the Kessler Medical Rehabilitation Research and Education Corporation (KMRREC) for providing the facility in which to work.

REFERENCES

1. Rodgers, M.M., et al., *Biomechanics of wheelchair propulsion during fatigue*. Arch Phys Med Rehabil, 1994. **75**: p. 85-93.
2. Rodgers, M.M., et al., *Three-dimensional dynamic analysis of joint reaction forces and moments during wheelchair propulsion*. Clin Kinesiol., 1994. **47**: p. 98.
3. Rao, S., et al., *Three-Dimensional Kinematics of Wheelchair Propulsion*. IEEE Transactions on Rehabilitation Engineering, 1996. **4**(3): p. 152-9.

4. Boninger, M.L., et al., *Propulsion Patterns and Pushrim Biomechanics in Manual Wheelchair Propulsion*. Arch Phys Med Rehabil. 2002. 83: p. 718-723.
5. Costic, R.S., et al., *Joint compression alters the kinematics and loading patterns of the intact and capsule-transected AC joint*. J Orthop Res, 2003. 21(3): p. 379-85.
6. Remia, L.F., et al., *Biomechanical evaluation of multidirectional glenohumeral instability and repair*. Clin Orthop, 2003. 416: p. 225-36.
7. Gokeler, A., et al., *Quantitative analysis of traction in the glenohumeral joint. In vivo radiographic measurements*. Man Ther., 2003. 8(2): p. 97-102.
8. Curtis, K., et al., *Shoulder Pain in Wheelchair Users with Tetraplegia and Paraplegia*. Arch Phys Med Rehabil, 1999. 80: p. 453-57.
9. Subbarao, J.V., M.D. Klopstein, and R. Turpin, *Prevalance and Impact of Wrist and Shoulder Pain in Patients with Spinal Cord Injury*. The Journal of Spinal Cord Medicine, 1994. 18: p. 9-13.
10. Rasmussen, J., <http://www.anybodytech.com>.
11. van der Helm, F.C., et al., *ISB Recommendation on Definitions of Joint Coordinate System of Various Joints for the Reporting of Human Joint Motion - Part II: Shoulder, Elbow, Hand and Wrist*. Submitted to Journal of Biomechanics. Last revision January 14, 2004.
12. Rasmussen, J., Damsgaard, M., and M. Voigt. *Muscle recruitment by the min/max criterion - a comparative numerical study*. Journal of Biomechanics. 2001. 34(3): p. 409-415.
12. Damsgaard, M., Christensen, S.T., and J. Rasmussen. *An efficient numerical algorithm for solving the muscle recruitment problem in inverse dynamics simulations*. International Society of Biomechanics, XVIIth Congress, July 8-13, 2001. Zurich, Switzerland.
13. Rasmussen, J., et al., *The role of mechanics and optimization in ergonomics*.
14. Damsgaard, M., Rasmussen, J., and S.T. Christensen. *Inverse dynamics of musculo-skeletal systems using an efficient min/max muscle recruitment model*. Proceedings of IDETC: 18th Biennial Conference on Mechanical Vibration and Noise. Pittsburgh, September 9-13, 2001.11.
15. Veeger, H.E.J., L.A. Rozendaal, and F.C. van der Helm, *Load on the shoulder in low intensity wheelchair propulsion*. Clin Biomech, 2002. 17(3): p. 211-8.
16. Helm, F.C.T. and V. H.E.J., *Quasi-static analysis of muscle forces in the shoulder mechanism during wheelchair propulsion*. J Biomech, 1996. 29: p. 39-52.